PROCEEDINGS, 42nd Workshop on Geothermal Reservoir Engineering
Stanford University, Stanford, California, February 13-15, 2017
SGP-TR-212

An Improved 2 m Survey Device and Its Application in Southeast Fujian in China

ZHANG Yanjun, XIE Yangyang, YU Ziwang, HU Zhongjun, ZHANG Tong

Mailing address: College of Construction Engineering, Jilin University 938 Ximinzhu Street, Changchun 130026, China

E-mail address: zhangyanj@jlu.edu.cn, xie_yangyang@foxmail.com

Keywords: shallow measurement, geothermal survey, improved device.

ABSTRACT

Preliminary geothermal surveys to identify areas of potential geothermal anomalies are the most important stage in traditional hydrothermal-type geothermal resource exploration procedures. Temperature gradient wells are limited because of their accessibility issues and high costs, whereas the 2 m survey is considered a rapid, efficient, and inexpensive method to measure temperature accurately and allow for rapid vectoring toward geothermal anomalies in cases where thermal groundwater is not overlain by near-surface cold aquifers. An improved quick and portable measurement device is developed that adds in situ thermal conductivity tests based on temperature. The device, which is easy to assemble, portable, and suitable for two or three people in field work, had been calibrated by laboratory experiments. This study will use this improved survey device in Xiamen City in China and combine an in situ thermal conductivity analysis with a temperature inverse forecast to increase preliminary geothermal survey accuracy and provide survey experience for other similar potential geothermal fields in China.

1. INTRODUCTION

Geothermal energy is a competitive type of clean renewable energy. Traditional hydrothermal-type geothermal resource exploration procedures usually include the following stages: (1) the preliminary survey stage, where surface anomalies are investigated (including hot springs, fumaroles, and salt tufa), after which geothermal areas are identified by comprehensive judgment of small-scale geological data and remote sensing data. (2) The geophysical and geochemical exploration stages, where magnetotelluric and controlled source audiomagnetotellurics or other methods are used in potential areas to continue to narrow the scope and determine the drilling positions (Kana et al. 2015). (3) The drilling survey stage, where temperature gradient wells are drilled to verify whether geothermal reservoirs exist. Generally, as each stage progresses, the economic cost will correspondingly increase to a higher level, particularly in the drilling stage, which requires a substantial cost but obtains limited temperature data by restricted boreholes (Zehner et al. 2012). The preliminary survey stage is the most important but is also the most challenging. During the preliminary stage, drilling is still the current most accurate method of identifying a potential geothermal anomaly area (Aretouyap et al. 2016). Although this method can accurately obtain the temperature data of the underground soil in target depth, its high costs limit its frequency of application.

Shallow temperature measurement is a method of measuring shallow-depth ground temperatures to identify geothermal anomaly areas. Compared with traditional methods, shallow temperature measurement is cheaper, more effective, and can obtain substantial temperature data in a short period of time. The shallow measurement method was first used to depict the geothermal anomaly at the preliminary survey stage in Nevada (Olmsted 1977). Several 1 m surveys have been successfully conducted at various locations in the Great Basin (Trexler et al. 1982). In 2007, the shallow measurement method was significantly improved by Great Basin Center for Geothermal Energy and University of Nevada and the 2 m survey method was first proposed (Coolbaugh et al. 2007). Several geothermal fields (including Dead Horse Wells, Hawthorne Army Depot, and Terraced Hills) were successfully predicted and detected by this novel method (Kratt et al. 2010). Compared with traditional 1 m survey method, 2 m survey method, which is a new shallow measurement method, performs better in reducing environmental impact and reflects more real geothermal anomaly.

Shallow temperature measurements have not been more widely used in geothermal exploration in the past because they are usually time-consuming and not fully field-portable (Coolbaugh et al. 2007). The traditional measurement equipment was limited to vehicles, and the temperature sensors were separated by metal rods in soil to eliminate frictional interference; thus, the measurement would last for 1 h at every measurement position (Sladek et al. 2007). The main objectives of this work are as follows: (1) to develop an improved quick and portable measurement device that reduces survey time and is independent of vehicles; (2) to add in situ thermal conductivity tests based on temperature tests which calibrated by laboratory experiment to improve the accuracy of the 2 m method at the early survey stage; and (3) to enhance survey accuracy of geothermal area identification. This study will use this improved survey device in Xiamen City in China and combine an in situ thermal conductivity analysis with a temperature inverse forecast to increase preliminary geothermal survey accuracy and provide survey experience for other similar potential geothermal fields in China.

2. TESTING EQUIPMENT

2.1 Device Structure Design

2.1.1 Boring Device

The boring device comprises a walk-behind power plant, drill pipes, and a drill bit (Figure 1). The walk-behind power plant consists of a small gasoline engine (1E48F). The gasoline engine possesses a large torque and a low speed, and its maximum power is 2.2 kW with a

speed of 7,500 r/min. The drill pipes are made of hardened steel and were designed to use a hollow tube with an average length of 120 cm and a diameter of 10 mm in each pipe. Two pairs of nail holes are designed in both sides of the drill pipe to allow convenient connection with the walk-behind power plant or the next pipe. The auger drill bit is selected for its efficient drilling capability. The drill bit is made of a hard alloy to ensure that it can drill in most conditions. The boring device can be dismantled, stored in a suitcase, and easily transported.

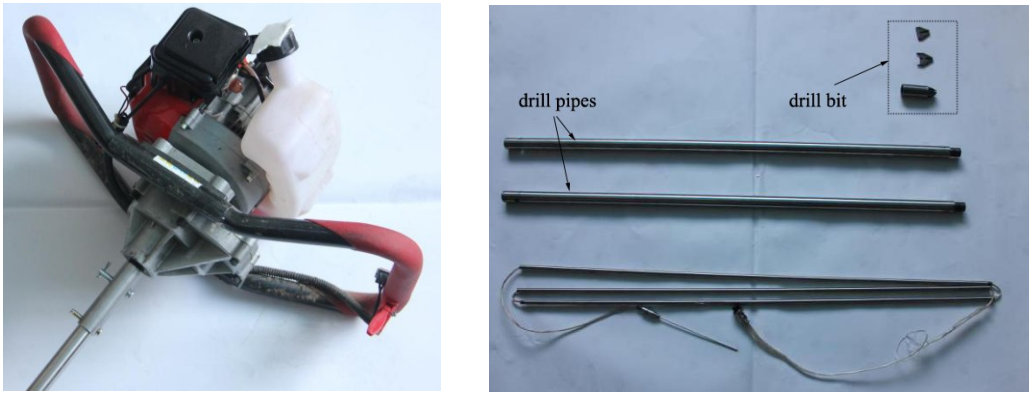

(a) (b)

Figure 1: The boring device comprises three parts, including (a) walk-behind power plant and (b) drill pipes and drill bit.

2.1.2 Measuring Probe

A large length-to-diameter ratio is designed for the probe to keep the soil samples in the unbounded heat-conducting media relative to the probe and to avoid axial heat conduction. Thus, the diameter of the probe is 2 mm and the length of the probe is 200 mm. The probe is designed in a small volume so that the thin but long probe can be easily inserted into the ground. In this case, the insertion procedure causes limited influence on the underground temperature field. The probe is composed of a needle tip, a stainless steel seamless slimline pipe, and a pin cap (Figure 2).

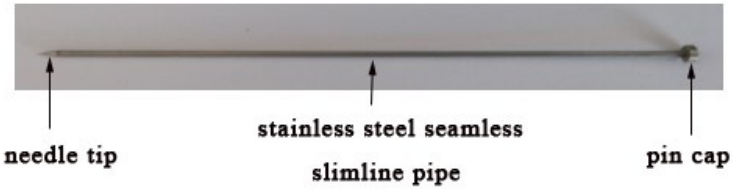

Figure 2: The 200 mm-long measure probe exhibits a diameter of 2 mm. It features three basic components, namely, a needle tip, a stainless steel seamless slimline pipe, and a pin cap.

2.1.3 Measuring Probe

The temperature acquisition microcontroller is a 16 bit MCU (MSP430F5438) made by Texas Instruments® (TI®). The *I–V* conversion circuit is designed to transform the PT1000 resistance variation into temperature data for storage in the programmable logic controller (PLC). The analog-to-digital converter (ADC) is ADS1240, which was also made by TI®. The measurement circuit is made by REF50xx. A battery is used to supply the power for the MCU, PLC, ADC and measurement circuit. The entire receiving device is sealed in a small electrical panel box (Figure 3). A software we composed by C# is used to process the data. The original data can be logged in the PLC and then introduced into the software in a tablet or PC. The data receiving device can be controlled by keyboard and touchscreen.

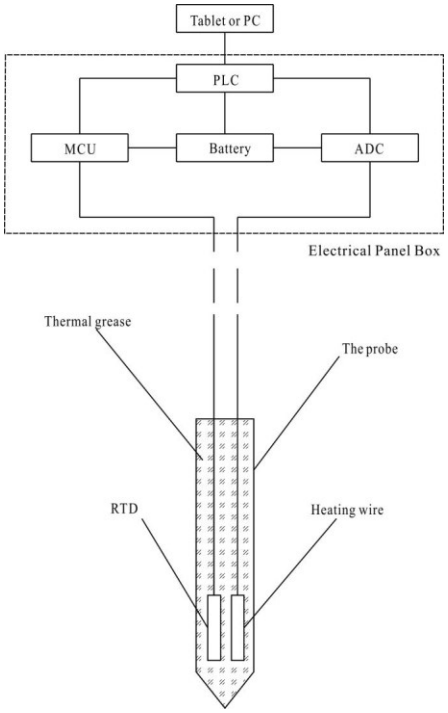

Figure 3: Design patterns of the data-receiving device.

2.1 Measurement Theoretical Basis

The measurement of thermal conductivity is based on needle probe method (Von Herzen and Maxwell 1959). The heat source model is based on unsteady heat conduction in unbounded media (Popov et al. 2012). Assuming that the underground soil mass is an unbounded heat-conducting media relative to the probe, the initial temperature of the layer is stable and the thermal parameters are constant as soil temperature fluctuates. The probe can be regarded as a line heat source. Heat conduction is a one-dimensional axisymmetric problem around the probe. According to the above assumptions, the distribution function of surplus temperature fields can be deduced from primitive equations (Carslaw and Jaeger 1959) and simplified as follows:

$$\theta = t - t_0 = \frac{-\mathrm{q}}{4\pi\lambda} E_i\left[-\frac{r^2}{4\mathrm{a}\tau}\right] \tag{1}$$

Where θ is the surplus temperature; t is the temperature at time τ; t_0 is the initial temperature; q is the heating power; λ is the soil thermal conductivity; E_i is the exponential integral function; r is the distance between a point and line heat source; a is the thermal diffusivity; and τ is the heating time. When r is sufficiently small and τ is sufficiently large, E_i can be calculated as follows:

$$E_i(-\mu) = C + \ln(\mu) \tag{2}$$

Where $\mu=r^2/4a$; C is Euler's constant, whose value is 0.57726. Equation (2) is substitute into Equation (1) and then the temperature of one point can be written as follows:

$$\theta_2 - \theta_1 = t_2 - t_1 = \frac{\mathrm{q}}{4\pi\lambda} \ln\frac{\tau_2}{\tau_1} \tag{3}$$

Equation (3) shows that lnτ and t possess a linear relationship. The curve of lnτ and t can be obtained by the least squares method. The relationship of lnτ and t can be defined as follows:

$$\ln\tau = \alpha_0 + \alpha_1 t \tag{4}$$

The sum of the deviation squares of lnt_i and lnτ$_i$ can be considered an optimal criterion. Thus, α_0 and α_1 can be calculated as follows:

$$\alpha_0 = \frac{\sum \ln\tau_i - \alpha_1 \sum t_i}{n} \quad (5)$$

$$\alpha_1 = \frac{n\sum t_i \ln\tau_i - \sum t_i \sum \ln \tau_i}{n\sum t_i^2 - \left(\sum t_i\right)^2} \quad (6)$$

The soil thermal conductivities (λ_i) can be calculated as follows:

$$\lambda_i = \frac{q}{4\pi} \frac{n\sum t_i \ln\tau_i - \sum t_i \sum \ln \tau_i}{n\sum t_i^2 - \left(\sum t_i\right)^2} \quad (7)$$

Based on the previously presented principles, the temperature of the soil sample can be measured immediately after the probe is inserted into the soil. When the thermal conductivity is measured, the measurement circuit opens and the heating wire and the temperature sensor begin to work. Timing when τ=0, and the time of temperature collection is recorded. The thermal conductivity (λ_i) at time τ_i is calculated by using Equation (7). The tablet or computer can display the variation curves of the thermal conductivity of soil.

3. LABORATORY CALIBRATION OF THE EQUIPMENT

The improved device was tested in a laboratory before being used in the field. Another controlled test was used as a comparison. The control group was tested by QTM, which is a typical thermal conductivity equipment in laboratory experiments. In the laboratory experiment, the tests were applied in three kinds of soil samples, namely, coarse sand (CS), fine sand (FS) and silty clay (SC). The three remolded samples were tested in varying levels of water content. At the beginning, the soil samples were dried to constant weight in a vacuum oven. Then, the dehydrated samples were saturated by adding distilled water with 2% to 5% of the gradient until the samples were saturated.

The measuring probe and QTM are used to measure every soil sample to verify the results of thermal conductivity obtained by the measuring probe. Temperature sensors placed around the soil sample box showed that the heat emitted by the probe would not affect the edge of soil samples. Thus, the soil samples are unbounded heat-conducting media relative to the probe. The measuring probe was inserted into the middle of the soil sample and heated with different work voltages for the same sample. Regardless of the voltage applied, the heating time was fixed at 150 s.

The tendency of thermal conductivity to vary among soil samples can be observed clearly based on the relationship between soil thermal conductivity and heating time depicted in Figure 4. The soil thermal conductivity surged drastically at the beginning, but as the heating time elapsed, the degree of the variation decreased gradually. Eventually, the variation of soil thermal conductivity almost stopped. When the variation tendency was stable, the result of soil thermal conductivity was considered close to the real value. Thus, the final result was selected based on the time for which the thermal conductivity remained stable and was calculated by the least squares method. Each soil sample was measured five times, and the average value was used as the value of the thermal conductivity of the soil samples by both devices.

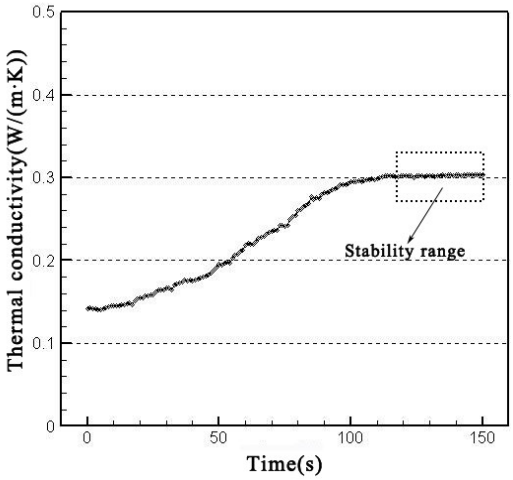

Figure 4: Thermal conductivity of coarse sand sample with 2% water content measured by probe in 9 V work voltage.

No failure data appeared according to the measurement report of soil samples in different water contents. The detailed results are shown in Table 1. Compared with the QTM results, in low water content, the thermal conductivity deviations measured at 6 V were smaller by 3.2%, whereas those measured at 9 V were smaller by 2.0% than the results obtained by the QTM. With the increase in water content, the deviations for samples heated with 6 V work voltage were smaller by 0.5% on average, whereas the deviation for samples heated with 9 V work voltage were larger by 1.6% on average.

Table 1 Thermal conductivity result of soil samples estimated by both QTM and measure probe.

No	sample code	water content	QTM	measure probe(6V)			measure probe(9V)		
				thermal conductivity	temperature vary	stable time	thermal conductivity	temperature vary	stable time
		%	W/m·K	W/m·K	℃	s	W/m·K	℃	s
1	CS00	0	0.282	0.255	8	82	0.273	15	104
2	CS02	2	0.315	0.293	8	90	0.303	13	118
3	CS04	4	0.398	0.362	5	80	0.37	9	95
4	CS06	6	0.858	0.828	6	85	0.849	11	105
5	CS08	8	1.047	1.045	7	95	1.105	14	120
6	CS10	10	1.528	1.581	8	90	1.612	15	115
7	CS12	12	2.052	1.988	8.5	95	2.042	14	125
8	CS16	16	2.263	2.313	7	80	2.291	13	120
9	FS00	0	0.216	0.198	7	95	0.201	13	100
10	FS02	2	0.226	0.207	8	100	0.211	14	120
11	FS04	4	0.34	0.358	8	90	0.342	12	115
12	FS06	6	0.533	0.544	8.5	96	0.547	11.5	110
13	FS08	8	0.65	0.654	9	112	0.668	12	124
14	FS10	10	0.755	0.723	9.3	110	0.75	10	110
15	FS13	13	0.858	0.832	9.5	115	0.897	14	120
16	FS16	16	1.136	1.135	8.8	95	1.178	13	125
17	FS20	20	1.365	1.381	9	90	1.401	12	115
18	FS25	25	1.47	1.456	7	98	1.493	13	120

19	SC00	0	0.216	0.215	7	90	0.215	12	120
20	SC03	3	0.281	0.274	8	97	0.283	13	115
21	SC07	7	0.435	0.434	8.5	95	0.432	12	125
22	SC11	11	0.835	0.854	8	90	0.837	11	120
23	SC15	15	1.254	1.245	7.5	100	1.265	12	124
24	SC20	20	1.365	1.353	7	96	1.37	13	120
25	SC25	25	1.57	1.535	8	100	1.573	12	125

4. FIELD EXPERIMENT IN XIAMEN CITY

4.1 Study Area and Experimental Design

Xiamen City is located in the southeastern area of Fujian Province in China and lies 1.5° north of the Tropic of Cancer, which possesses a marine monsoon climate with abundant precipitation and sunshine. The field experiment area in Dongshan is located northeast of Xiamen City (Figure 5). The annual average temperature of Dongshan is 21 ℃ with no evident division among the four seasons. The surface terrain of Dongshan is gentle, and its geographical feature is simple. The land is mainly covered by alluvial soil and diluvium soil during the Quaternary Period. The water table of the field experiment area is high, and its depth ranges from 0.3 m to 5 m.

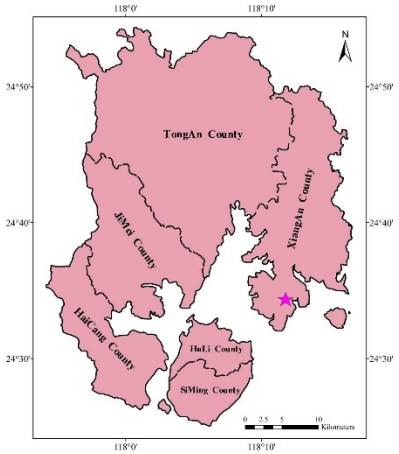

Figure 5: Location of the Dongshan geothermal field in Xiamen.

The field survey data are collected by the Geological Engineering Investigation Institute of Xiamen City. Monitoring wells and measurement wells are drilled to obtain a general idea of the location of geothermal anomalies and the temperature details in shallow underground. Areas with geothermal anomalies exhibit an elliptical or irregular circle loop shape. The potential geothermal anomaly area covers an area of approximately 0.4 km^2, and two spring spots are traced. Based on the experience of shallow (1 m to 2 m) temperature measurements in New Zealand (Thompson 1964), 18 measurement positions are arranged divergent in distance according to the two spring spots in the potential geothermal anomaly area.

The measurement positions are adjusted properly to avoid the ponds or surface runoff areas. The shallow soil is mainly covered by clay. The boring device is used to drill the borehole and the probe is inserted into the hollow drill pipes to the target depth. The device measures the temperatures at the depths of 1 and 2 m and the in situ thermal conductivity for all the 18 measurement positions on November 14 and 15, 2014 when the climate was stable with the lowest rainfall in a year. Meanwhile, the altitude and geographic coordinates are recorded by GPS. Given that all measurements were completed within two days, the temperature variety caused by climate was negligible. Therefore, seasonal correction of the temperature data need not be conducted.

4.2 Results and Discussion

4.2.1 Temperature Anomaly Area Identification

During temperature measurement, the probe should be inserted into the soil and the measurement should last 5-10 min for temperature equilibrium to avoid the influence of the disturbance caused by drilling. If the temperature sensor remains stable for at least 300 s, then the temperature is recorded for this position. The temperature nephogram for the Dongshan geothermal anomaly area is plotted by the method of interpolation shown in Figure 6 according to the 2 m survey data. Temperature data provided by the 2 m measurement allows the resolution of the potential geothermal area into two separate anomalies, namely, a weak, narrow western anomaly with peak 2 m temperatures of 24°C to 25 °C and a stronger, broad eastern anomaly with peak 2 m temperatures of 32°C to 33 °C.

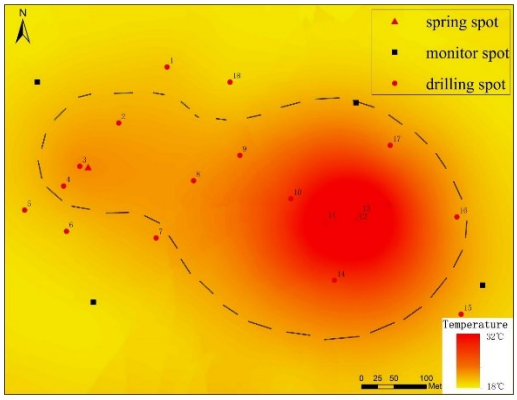

Figure 6: Temperature nephogram at 2 m depth of Dongshan geothermal field. The dotted-line region represents anomaly area.

4.2.2 Thermal Conductivity and Thermal Flux

The water table and in situ thermal conductivity measured at the depths of 1 and 2 m are shown in Figure 7. Several correlations show that increases in falling water tables decrease the thermal conductivity for both depths, and vice versa. These results are consistent with the theoretical explanation that conducting conditions are poor because the soil pores are filled with air. Given that the thermal conductivity of water and air are 0.6W/(m·K) and 0.024W/(m·K) in the standard case (Yuan et al. 2010), respectively, replacing air with water decreases the thermal contact resistance because water forms an aqueous film between soil particles, thus increasing thermal conductivity.

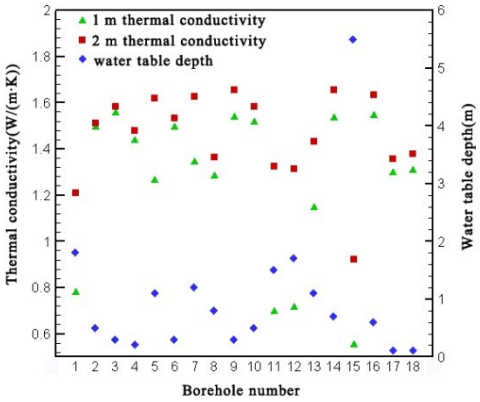

Figure 7: Scatter diagram of 1 m thermal conductivity, 2 m thermal conductivity, and water table.

Divided from the water table, the underground soil can be simplified into the saturated soil layer and the unsaturated soil layer. Meanwhile, the two parts have different levels of thermal conductivity. The interpolation method is used to calculate the integrated thermal conductivity if the water table is deeper than 1 m but less than 2 m. Using the temperature difference between 1 m and 2 m depths as the temperature gradient, the shallow thermal flux can be calculated by the grid data of temperature and integrated thermal conductivity. The shallow thermal flux nephogram is depicted in Figure 8. The shallow thermal flux distribution basically matches the temperature nephogram that shows two geothermal flux peaks. Compared with temperature distribution, analyses that combine thermal flux distribution will reveal more about the tendency of geothermal anomalies to vary. Thus, geothermal centers are more accurately depicted and survey accuracy is improved.

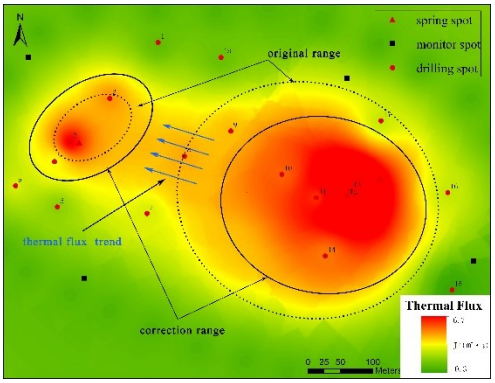

Figure 8: Thermal flux nephogram at 2 m depth of Dongshan geothermal field. The original and correction-affected regions are shown. The transit tendency of the thermal flux is strong from east to west.

4.2.3 Correction Geothermal Effect Range

Based on the temperature difference between anomaly threshold temperature and 2 m temperature, if the anomaly threshold temperature is defined in 20.0 °C (the average temperature of surface from previous monitoring data), then the anomaly range can be distinguished beyond a distance of 190 m (Figure 9a) apart from the eastern anomaly center. However, only distance differentials of 70 m (Figure 9a) can be distinguished from the western anomaly center. Surface temperatures are easiest to measure and can be mapped in detail with thermal remote sensing. But thermal remote sensing is strongly influenced by solar radiation, vegetation, and climate, which make it an unreliable stability criterion (Coolbaugh et al. 2007). However, the environmental influence decreases significantly in the 1 m depth temperature (Jia et al. 1986); thus, the correction geothermal affect range of the anomaly center is depicted by the difference between 2 m measure temperature and 2 m derivation temperature. The 2 m derivation temperature is calculated by 1 m temperature and in situ thermal conductivity. The correction geothermal affect range is distinguished in Figure 9b. As the distance between anomaly center and borehole increases, the temperature difference decreases. Two correction affect regions are shown in the geothermal area, namely, a broad eastern affect range with a conspicuous temperature difference in the radius of 150 m and a slightly smaller western affect range in the radius of 100 m.

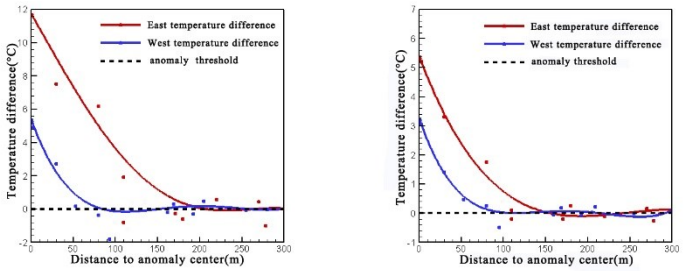

(a) (b)

Figure 9: (a) Temperature difference between 2 m and anomaly threshold temperature. (b) Temperature difference between 2 m and 2 m derivation temperature.

4.2.4 The 20 m Depth Temperature Inversion Forecast

Temperatures at depths >20 m are unaffected by the surface environment, and at these depths, recognizing and mapping a geothermal area becomes easier (LeSchack and Lewis 1983). Environmental influence evidently decreases when the depth increases if the measurement is conducted below the depth of 1 m; thus, the underground temperature field deeper than 2 m can be approximately regarded as a steady temperature field. Based on this hypothesis, the underground temperature inversion model will be simplified as follows: (1) underground heat transfer occurs only as a form of heat conduction, ignoring heat convection and heat radiation; (2) the heat energy around the borehole transfers only along the drill direction, which belongs to a unidirectional heat conduction model; (3) throughout the process of heat conduction, the heat flow density from every layer is regarded as invariant or the lateral heat dissipation in each layer is ignored; (4) the thermal conductivity of every layer will not change with the variation in temperature or other factors. According to these simplified conditions, utilized the 2 m temperature data and integrated thermal conductivity, the 20 m temperature could be inversed by the Fourier Law.

The geothermal anomaly area is generally divided into three districts by stratum data shown in Figure 10. In district I, the soil from the surface to 4 m in depth comprises clay, sandy clay, and silt; soil from 4 m to 20 m is composed of sandy clay. In district II, soil at depths of 0 m to 4 m comprises clay, sandy clay, and silt; soil from 4 m to 16 m deep comprises sandy clay; and soil 16 m to 20 m deep comprises granite. In district III, soil from 0 m to 4 m deep comprises clay, sandy clay, and silt; soil 4 m to 10 m deep comprises sandy

clay; and soil 10 m to 20 m comprises granite. Except for Boreholes 3, 4, 6, 7, and 8, which are located in district III, all boreholes are located in district II. Based on the integrated thermal conductivity calculated by in situ measurement and laboratory tests, the 20 m temperature can be inversed using the steady-state heat conduction model

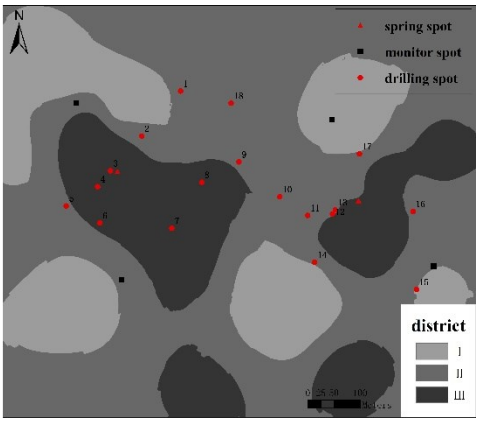

Figure 10: Stratigraphic regionalization of Dongshan geothermal field.

According to the inversion data, the eastern geothermal center exhibited a temperature of 68.75 °C and the western geothermal center exhibited a temperature of 45.91 °C at a depth of 20 m. The average temperature error of all 18 boreholes at a 20 m depth is 3 °C, whereas the relative error between actual and forecast values is less than 10%. The relationship between actual value and forecast value plotted together is $R^2 = 0.92859$ (Figure 11).

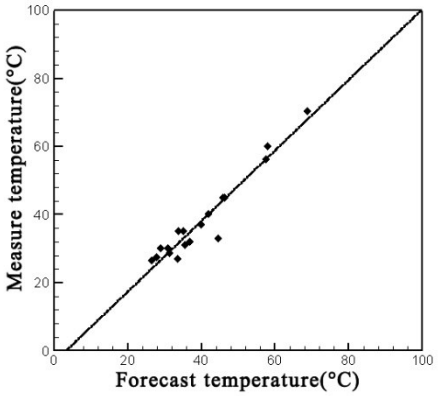

Figure 11: Correlation analysis between measured and forecast values of temperature.

5. CONCLUSION

In this work, an improved device for 2 m survey has been developed. The entire setup weighs no more than 20 kg, is easy to assemble, is portable, and is suitable for a team of two or three individuals. The device adds in situ thermal conductivity measurement by the needle probe method based on original temperature measurements. The probe method has the advantages of small contact size and a short balancing time. Thus, temperature and thermal conductivity can be accurately measured by minimum impact in less than 10 min for every borehole. The 2 m survey result of the field experiment in Dongshan geothermal field can be used to describe the geothermal anomaly in the area. Compared with the costly and time-consuming drilling survey during the preliminary stage of exploration, the 2 m survey with the improved device can provide reliable survey results. The successful identification of a potential geothermal anomaly area at Dongshan geothermal field demonstrates how 2 m temperature measurements can reduce the costs of geothermal exploration programs and increase their efficiency. Furthermore, they provide a greater likelihood of success in locating thermal anomalies in the preliminary stage of exploration. The comparison of actual values collected by drilling data with inverse forecast values demonstrates a strong correlation, which indicates that the 2 m survey is an effective initial geothermal survey method. Based on the 2 m survey results in the preliminary survey stage, temperature measurement wells can be more rationally sited in potential geothermal anomaly areas so that they can optimize drilling, reduce surveying length, and enhance returns in the subsequent stage.

ACKNOWLEDGMENTS

This study was supported by the National High Technology Research and Development Program of China (863 Program) (No. 2012AA052803), the Natural Science Foundation of China (Grant No. 41372239). Some of the data set has been provided by Geological Engineering Investigation Institute of Xiamen City.

REFERENCES

Aretouyap Z, Nouck PN, Nouayou R (2016) A discussion of major geophysical methods used for geothermal exploration in Africa. Renew Sustain Energy Rev 58:775–781

Carslaw HS, Jaeger JC (1959) Conduction of heat in solids. Clarcdon Press, Oxford

Coolbaugh M, Sladek C, Faulds J, Zehner R, Oppliger G (2007) Use of rapid temperature measurements at a 2-meter depth to augment deeper temperature gradient drilling. In: Thirty-second workshop on geothermal reservoir engineering

Jia L, Guan X, Xu J (1986) An investigation into some problems of one meter thermometry in geothermal exploration. Geophys Geochem Explor 10(2):115–122

Kana JD, Djongyang N, Raïdandi D et al (2015) A review of geophysical methods for geothermal exploration. Renew Sustain Energy Rev 44:87–95

Kratt C, Sladek C, Coolbaugh MF (2010) Boom and bust with the latest 2 m temperature surveys: Dead Horse Wells, Hawthorne Army Depot, Terraced Hills and other areas in Nevada. Geotherm Resour Counc Trans 34:567–574

LeSchack LA, Lewis JE (1983) Geothermal prospecting with ShalloTemp surveys. Geophysics 48:975–996

Olmsted FH (1977) Use of temperature surveys at a depth of 1 meter in geothermal exploration in Nevada. United States Geological Survey Professional Paper, 1044-B, 25

Popov Y, Bayuk I, Parshin A (2012) New methods and instruments for determination of reservoir thermal properties. In: Proceedings, thirty-seventh workshop on geothermal reservoir engineering, Stanford University, Stanford, California

Sladek C, Coolbaugh MF, Zehner RE (2007) Development of 2-meter soil temperature probes and results of temperature survey conducted at Desert Peak, Nevada, USA. Geotherm Resour Counc Trans 31:363–368

Thompson GEK (1964) Proceedings of United Nations Conference on New Sources of Energy, vol 2, pp 386–401

Trexler DT, Koenig BA, Ghusn G Jr, Flynn T, Bell EJ (1982) Lowto-moderate-temperature geothermal resource assessment for Nevada: area specific studies, Pumpernickel Valley, Carlin and Moana. United States Department of Energy Geothermal Energy Report DOE/NV/10220-1 (DE82018598)

Von Herzen V, Maxwell AE (1959) The measurement of thermal conductivity of deep-sea sediments by a needle-probe method. J Geophys Res 64(10):1557–1563

Yuan XZ, Li N, Zhao XY et al (2010) Study of thermal conductivity model for unsaturated unfrozen and frozen soils. Rock Soil Mech 31(9):2089–2694

Zehner RE, Tullar KN, Rutledge E (2012) Effectiveness of 2-meter and geoprobe shallow temperature surveys in early stage geothermal exploration. Geotherm Resour Counc Trans 36:835–842